Frascati Physics Series Vol. XXXVII (2004) pp. 397–411
Frontier Science 2004, Physics and Astrophysics in Space
Frascati, 14-19 June, 2004

SPECTRUM FEATURES OF UHE PROTONS INTERACTING WITH CMB

V. Berezinsky

INFN, Laboratori Nazionali del Gran Sasso,67010 Assergi (AQ), Italy

Abstract

UHE extragalactic protons propagating through cosmic microwave background radiation (CMB) acquire the spectrum features in the form of the dip, bump and the Greisen-Zatsepin-Kuzmin (GZK) cutoff. The GZK cutoff is a steepening of the spectrum which occurs due to pion production in collisions with CMB photons. The GZK steepening is a model-dependent feature: it can be more flat in case of local overdensity of the sources and more steep in case of the local deficit. The protons do not disappear in interaction with CMB. They are only shifted to low energies and produce the *bump* of pile-up protons there. This *bump* is distinctly seen in the spectra of single sources, but since the bumps are located at different energies, they disappear in the diffuse spectra. The *dip* is produced due to e^+e^- pair-production in collision of protons with CMB photons. This feature is weakly model-dependent and is reliably predicted. The predicted dip is distinctly seen in the observational data, and thus it becomes the confirmed signature of UHE extragalactic protons propagating through CMB.

1 Introduction

The nature of signal carriers of UHECR is not yet established. The most natural primary particles are extragalactic protons. Due to interaction with the CMB radiation the UHE protons from extragalactic sources are predicted to have a sharp steepening of energy spectrum, so called GZK cutoff [1]. For uniformly distributed sources, the GZK cutoff is characterized by energy $E_{1/2}$, where the integral spectrum calculated with energy losses taken into account becomes twice lower than the power-law extrapolation from low energies [2] $E_{1/2} = 5.7 \times 10^{19}$ eV.

There are two other signatures of extragalactic protons in the spectrum: dip and bump [3, 2, 4, 5]. The dip is produced due $p + \gamma_{\rm CMB} \rightarrow p + e^+ + e^-$ interaction at energy $E \sim 1 \times 10^{19}$ eV. The bump is produced by pile-up protons which loose energy in the GZK cutoff. As was demonstrated in [2], see also [5], the bump is clearly seen from a single source at large redshift z, but it practically disappears in the diffuse spectrum, because individual peaks are located at different energies. We shall demonstrate here that what is seen now in the observed spectrum as a broad bump is an artifact caused by multiplication of the spectrum to E^3.

A reliable feature in UHE proton spectrum is the dip produced by e^+e^- pair creation on CMB photons. It is less model dependent than GZK feature. Being relatively faint feature, it is however clearly seen in the spectra observed by AGASA, Fly's Eye, HiRes and Yakutsk arrays and can be considered as the confirmed signature of interaction of extragalactic UHE protons with CMB. This feature will be discussed in detail in this paper. The measurement of the atmospheric height of EAS maximum, $x_{\rm max}$, in the HiRes experiment (see Fig.1) gives another evidence of pure proton composition at $E \geq 1 \times 10^{18}$ eV. Yakutsk data also favour the proton composition at $E \geq 1 \times 10^{18}$ eV [6], though the other methods of mass measurements show the mixed chemical composition [7].

At what energy the extragalactic component sets in?

According to the KASCADE data [8], the spectrum of galactic protons has a steepening at $E \approx 2.5 \times 10^{15}$ eV (the first knee), helium nuclei - at $E \approx 6 \times 10^{15}$ eV, and carbon nuclei - at $E \approx 1.5 \times 10^{16}$ eV. It confirms the rigidity-dependent confinement with critical rigidity $R_c = E_c/Z \approx 3 \times 10^{15}$ eV. Then galactic iron nuclei are expected to have the critical energy of confinement at $E_c \sim 1 \times 10^{17}$ eV, and extragalactic protons can naturally dominate at $E \approx 1 \times 10^{18}$ eV. This energy is close to the energy of the second knee (Akeno - 6×10^{17} eV, Fly's Eye - 4×10^{17} eV, HiRes - 7×10^{17} eV and Yakutsk - 8×10^{17} eV). The detailed analysis of transition from galactic to extragalactic component of CR is given in [9]. It favours the transition at $E \sim 1 \times 10^{18}$ eV. The model of galactic cosmic rays developed by Biermann et al [10] also predicts the second knee as the "end" of galactic cosmic rays (iron nuclei) due to rigidity bending in wind-shell around SN. The extragalactic component became the dominant one at energy $E \sim 1 \times 10^{18}$ eV (see Fig.1 in [10]). The good candidates for the sources of observed UHE protons are

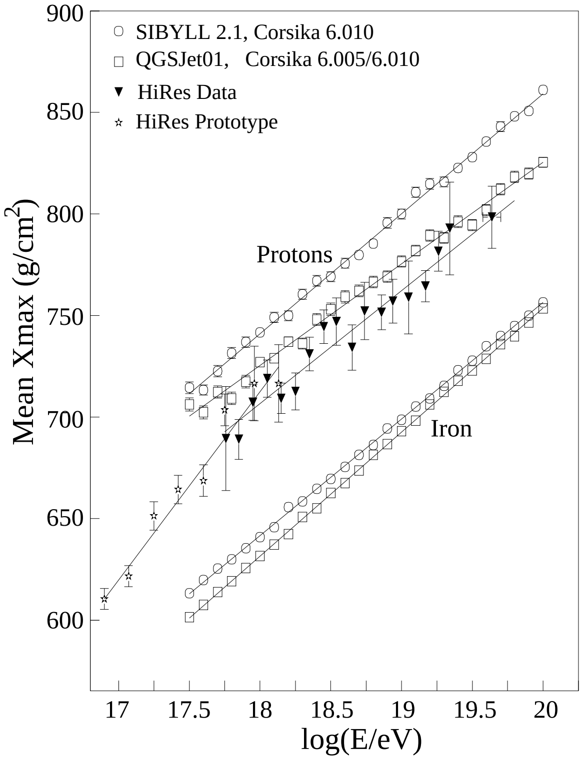

Figure 1: The HiRes data [11] on mass composition. The measured $x_{\max}$ at $E \gtrsim 1 \times 10^{18}$ eV (triangles) are in a good agreement with QGSJet-Corsika prediction for protons.

AGN. They can accelerate protons up to energy $E_{\max} \sim 10^{21}$ eV [12, 13, 14], they have power to provide the observed flux of UHE protons [15] and finally there observed the direct correlations [16] between directions of arrival of UHE particles with energies $(4-8) \times 10^{19}$ eV and directions to BL Lacs, which comprise some particular class of AGN.

Does it mean that UHECR puzzle has been already resolved in most conservative way?

In this model AGN cannot be the sources of observed particles with energy $E \geq 1 \times 10^{20}$ eV [17]: the attenuation length for a proton of this energy is smaller than 135 Mpc, and correlation with AGN would be seen for all these particles, contrary to observations. The particles observed at $E \geq 1 \times 10^{20}$ eV, in particular those detected in AGASA, imply the presence of another component, e.g. produced by decays of superheavy DM.

2 $E_{1/2}$ as characteristic of the GZK cutoff.

$E_{1/2}$ is the energy where the flux calculated with energy losses becomes twice less than power-law extrapolation of integral spectrum. In Fig.2a the function $E^{(\gamma-1)}J(>E)$ is plotted as function of energy ($\gamma > \gamma_g$ is the effective index). For wide range of generation indices $2.1 \leq \gamma_g \leq 2.7$ the cutoff energy is the same, $E_{1/2} \approx 5.7 \times 10^{19}$ eV. We have determined $E_{1/2}$ from the Yakutsk data.

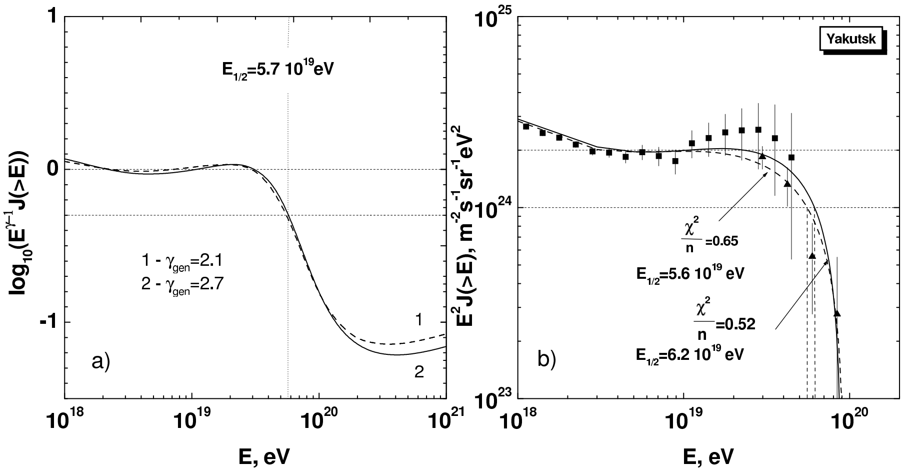

Figure 2: $E_{1/2}$ as numerical characteristic of the GZK cutoff. In panel a) the calculations for different γ_{gen} are presented. In panel b) $E_{1/2}$ is found from the integral spectrum of the Yakutsk array using two fits of the integral spectrum.

For this we found two fits of the Yakutsk integral spectrum with help of trial functions, as shown in Fig.2b. They have good χ^2/n equal to 0.65 and 0.52 (n is number of d.o.f.). The corresponding values of $E_{1/2}$, 5.6×10^{19} eV and 6.2×10^{19} eV, agree well with the theoretical value. Note, that in the fits above χ^2/n are the formal values from which probabilities cannot be calculated in the standard way, because the points in the integral spectrum are correlated quantities.

This analysis cannot be extended to the AGASA integral spectrum, because of too many events at the highest energies. Unfortunately, we do not have the

HiRes integral spectrum to perform the analysis as that above.

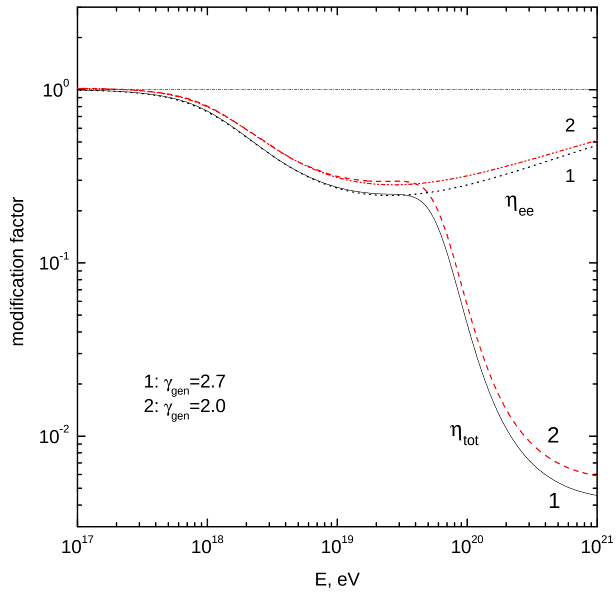

Figure 3: Modification factor for the power-law generation spectra with γ_g in a range 2.0 -2.7. Curve $\eta = 1$ corresponds to adiabatic energy losses only, curves η_{ee} corresponds to adiabatic and pair production energy losses and curves $\eta_{\rm tot}$ - to all energy losses included.

3 Bump in the diffuse spectrum

The analysis of the bump and dip is convenient to perform in terms of *modification factor* [2].

The modification factor is defined as a ratio of the spectrum $J_p(E)$, with all energy losses taken into account, to unmodified spectrum $J_p^{\rm unm}$, where only adiabatic energy losses (red shift) are included.

$$\eta(E) = \frac{J_p(E)}{J_p^{\rm unm}(E)}. \tag{1}$$

For the power-law generation spectrum $\propto E_g^{-\gamma_g}$ from the sources without cosmological evolution one obtains the unmodified spectrum as

$$J_p^{\rm unm}(E) = \frac{c}{4\pi}(\gamma_g - 2)\mathcal{L}_0 E^{-\gamma_g} \int_0^{z_{\rm max}} dz \frac{dt}{dz}(1+z)^{-\gamma_g}, \tag{2}$$

where the observed energy E and emissivity $\mathcal{L}_0$ is measured in GeV and GeV/Mpc^{3}yr, respectively. The connection between dt and dz is given by usual cosmological expression. The flux $J_p(E)$ is calculated in [17] with all energy losses included. In Fig. 3 the modification factor is shown as function of energy for two spectrum indices $\gamma_g = 2.0$ and $\gamma_g = 2.7$. They do not differ much from each other because both numerator and denominator in Eq. (1) include factor $E^{-\gamma_g}$. Let us discuss first the bump. We see no indication of the bump in Fig. 3 at merging of $\eta_{ee}(E)$ and $\eta_{\rm tot}(E)$ curves, where it should be located. The absence of the bump in the *diffuse spectrum* can be easily understood. The bumps are clearly seen in the spectra of the single remote sources [2]. These bumps, located at different energies, produce a flat feature, when they are summed up in the diffuse spectrum. This effect can be illustrated by Fig. 4 from Ref. [2]. In Fig. 4 the diffuse flux is calculated in the model where sources are distributed uniformly in the sphere of radius $R_{\rm max}$ (or $z_{\rm max}$). When $z_{\rm max}$ are small (between 0.01 and 0.1) the bumps are seen in the diffuse spectra. When radius of the sphere becomes larger, the bumps merge producing the flat feature in the spectrum. If the diffuse spectrum is plotted as $E^3 J_p(E)$ this flat feature looks like a pseudo-bump.

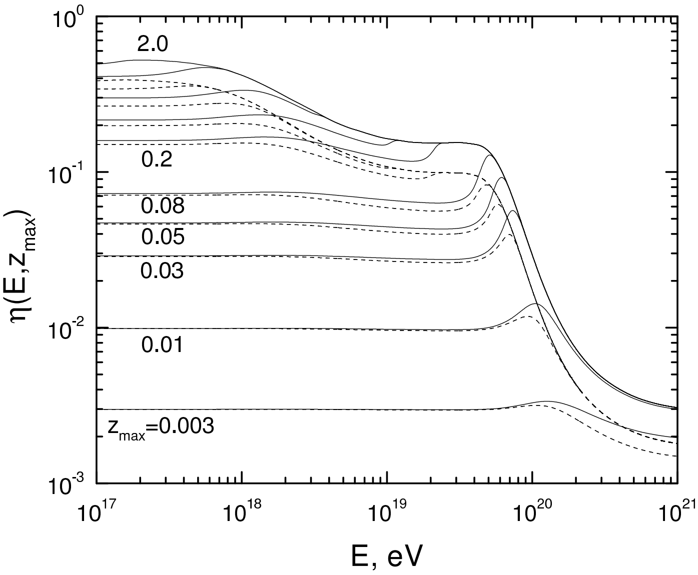

Figure 4: Disappearance of bumps in diffuse spectra (from Ref. [2]). The sources are distributed uniformly in the sphere of radius $R_{\rm max}$, corresponding to $z_{\rm max}$. The solid and dashed curves are for $\gamma_g = 2.7$ and $\gamma_g = 2.0$, respectively. The curves between $z_{\rm max} = 0.2$ and $z_{\rm max} = 2.0$ have $z_{\rm max} = 0.3,\ 0.5,\ 1.0$.

4 Dip as the signature of proton interaction with CMB.

The *dip* is more reliable signature of interaction of protons with CMB than GZK feature. The shape of the GZK feature is strongly model-dependent: it is more flat in case of local overdensity of the sources, and more steep in case of their local deficit. It depends also on fluctuations in the distances between sources inside the GZK sphere and on fluctuations of luminosities of the sources there. The shape of the *dip* is fixed and has a specific form which is difficult to

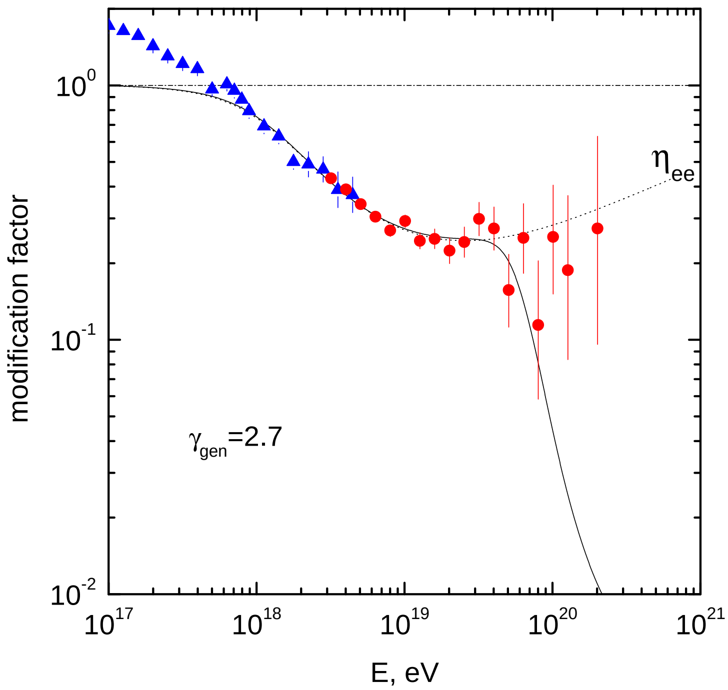

Figure 5: Predicted dip in comparison with the Akeno-AGASA data.

imitate by other mechnisms. The protons in the dip are collected from the large volume with the linear size about 1000 Mpc and therefore the assumption of uniform distribution of sources within this volume is well justified. In contrast to this well predicted and specifically shaped feature, the cutoff, if discovered, can be produced as the acceleration cutoff (steepening below $E_{\max}$). Since the shape of both, GZK cutoff and acceleration cutoff, is model-dependent, it will be difficult to argue in favour of any of them. The problem of identification of the dip depends on the accuracy of observational data, which should confirm the specific (and well predicted) shape of this feature. Do the present data have the needed accuracy?

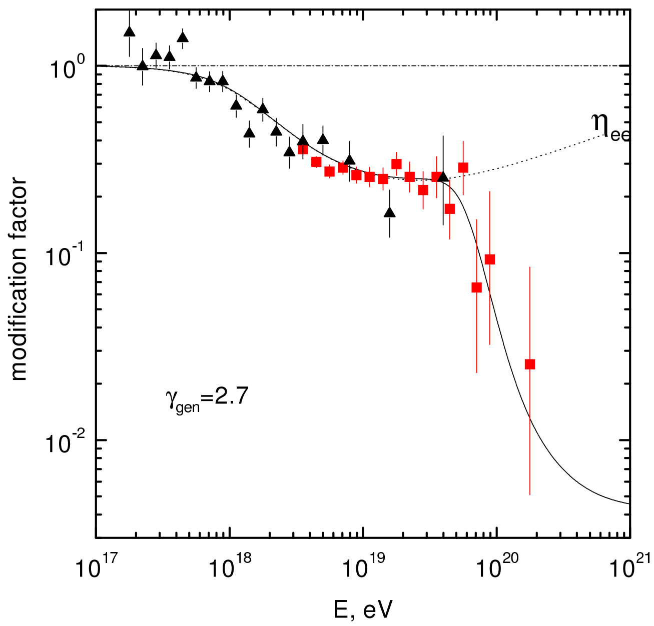

Figure 6: Predicted dip in comparison with the HiRes data.

The comparison of the calculated modification factor with that obtained from the Akeno-AGASA data, using $\gamma_g = 2.7$, is shown in Fig. 5. From Fig. 5 one observes the excellent agreement of predicted and observed modification factors for the dip.

In Fig. 5 one observes that at $E < 1 \times 10^{18}$ eV the agreement between calculated and observed modification factors becomes worse and at at $E \leq 4 \times 10^{17}$ observational modification factor becomes larger than 1. Since by definition $\eta(E) \leq 1$, it signals about appearance of another component of cosmic rays, which is most probably galactic cosmic rays. The condition $\eta > 1$ means the dominance of the new (galactic) component, the transition occurs at higher energy. To calculate χ^2 for the confirmation of the dip by Akeno-AGASA data, we choose the energy interval between 1×10^{18} eV (which is somewhat arbitrary in our analysis) and 4×10^{19} eV (the energy of intersection of $\eta_{ee}(E)$ and $\eta_{\rm tot}(E)$). In calculations we used the Gaussian statistics for low-energy bins, and the Poisson statistics for the high energy bins of AGASA. It results in $\chi^2 = 19.06$. The number of Akeno-AGASA bins is 19. We use in calculations two free parameters: γ_g and the total normalization of spectrum. In effect, the confirmation of the dip is characterised by $\chi^2 = 19.06$ for d.o.f=17, or χ^2/d.o.f.=1.12, very close to ideal value 1.0.

In Fig. 6 the comparison of modification factor with the HiRes data is shown. The agreement is also good.

The good agreement of the shape of the dip $\eta_{ee}(E)$ with observations is a strong evidence for extragalactic protons interacting with CMB. This evidence is confirmed by the HiRes data on the mass composition (see Fig. 1).

5 SuperGZK particles as a problem of astrophysical solution

The observed superGZK particles, i.e. those with energies higher than 1×10^{20} eV, impose a problem for astrophysical (acceleration) solution to origin of UHECR.

The "AGASA excess", namely 11 events with energy higher than 1×10^{20} eV, cannot be explained as extragalactic protons, nuclei or photons. While the spectrum up to 8×10^{19} eV is well explained as extragalactic protons with the GZK cutoff, the AGASA excess should be described as another component of UHECR, most probably connected with the new physics: superheavy dark matter, new signal carriers, like e.g. light stable hadron and strongly interacting neutrino, the Lorentz invariance violation etc.

The problem with superGZK particles is seen in other detectors, too. Apart from the AGASA events, there are five others: the golden FE event with $E \approx 3 \times 10^{20}$ eV, one HiRes event with $E \approx 1.8 \times 10^{20}$ eV and three Yakutsk events with $E \approx 1 \times 10^{20}$ eV. No sources are observed in the direction of these particles at the distance of order of attenuation length. The most severe problem is for the golden FE event: with attenuation length $l_{\rm att} = 21$ Mpc and the homogeneous magnetic field 1 nG on this scale, the deflection of particle is only 3.7°. Within this angle there are no remarkable sources at distance ~ 20 Mpc . SuperGZK particles can be explained by elementary-particle solutions, one of which is UHECR from Superheavy Dark Matter (SHDM), see reviews [18]. SHDM particles have masses $m_X \sim 10^{13}-10^{14}$ GeV. They are produced at post-inflationary epoch gravitationally, when the Hubble constant $H(t) \gtrsim m_X$. To be (quasi)stable these particles should be protected by some symmetry from the fast decay. The example of such symmetry is a gauge discrete symmetry, like e.g. R-parity in case of neutralino. As any other cold DM the SHDM particles are accumulated in the halo with overdensity $\sim 2 \times 10^5$, and hence UHECR produced at the decays of these particles do not have the GZK cutoff. The spectrum of the produced UHE particles are nowdays reliably calculated. Since m_X is basically determined by cosmologigal density of SHDM Ω_m known from WMAP measurements, the only free parameter of the model is life-time τ_X of X-particles. Varying τ_X one can change the absolute flux of UHECR from SHDM, i.e. the normalization. In Fig. 7 the flux of UHECR is shown as the sum of two components: the astrophysical flux, most probaly from AGN,

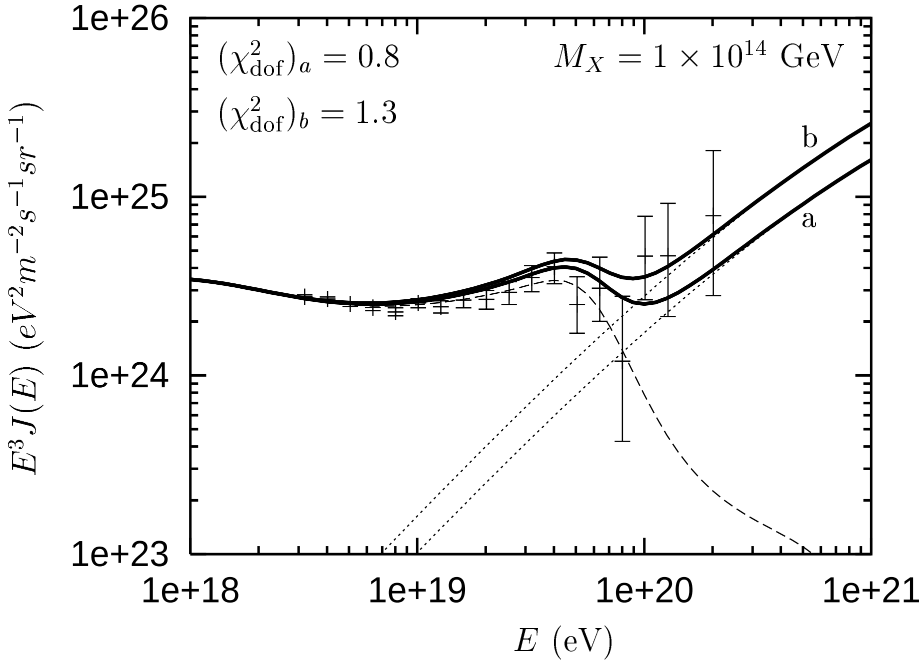

Figure 7: The astrophysical spectrum (dashed curve) and spectra from SHDM (dotted curves) [19], in comparison with AGASA data. The SHDM spectra are shown for two normalizations. The sum of two components is shown by the thick solid curves. The χ^2 values are given for the comparison of these two curves with the AGASA data at $E \geq 4 \times 10^{19}$ eV.

shown by dashed line and the flux from SHDM shown by dotted lines, according to calculations [19]. The AGASA spectrum, including the AGASA excess at $E \gtrsim 1 \times 10^{20}$ eV is well explained by the sum these fluxes shown by thick curves.

6 Conclusions

There are three signatures of UHE protons propagating through CMB: GZK cutoff, bump and dip.

The energy shape of the GZK feauture is very model dependent. The local excess of sources makes it flatter, and the deficit - steeper. The shape is affected by fluctuations of distances between the sources and of source luminosities. The cutoff, if discovered, can be produced as the acceleration cutoff (steepening below the maximum energy of acceleration). Since the shape of both, the GZK cutoff and acceleration cutoff, is model-dependent, it will be difficult to argue in favour of any of them.

The *bump* is produced by pile-up protons, which are loosing the energy in photopion interactions and are accumulated at low energy, where the photopion energy losses become as low as pair-production energy losses. Such a bump is distinctly seen in calculation of spectrum from a single remote source. In the diffuse spectrum, since the individual peaks located at different energies, a flat spectrum feature is produced.

The *dip* is most remarkable feature of interaction with CMB. The protons in this energy region are collected from the distances $\sim$ 1000 Mpc, with each radial interval dr providing the equal flux. All density irregularities and all fluctuations are averaged at this distance, and assumption of uniform distribution of sources with average distances between sources and average luminosities becomes quite reliable. The dip is confirmed by Akeno-AGASA and HiRes data with the great accuracy (see Figs 5 and 6). At energy $E > 4 \times 10^{19}$ eV the modification factor from Akeno data exceeds 1, and it signals the dominance of another CR component, most probably the galactic one. It agrees with transition of galactic to extragalactic component at the second knee $E \sim 1 \times 10^{18}$ eV.

How extragalactic magnetic field affects the calculated spectra features? The influence of magnetic field on spectrum strongly depends on the separation of the sources d. There is statement which has a status of the theorem [20]:

For uniform distribution of sources with separation much less than characteristic lengths of propagation, such as attenuation length $l_{\rm att}$ and the diffusion length $l_{\rm diff}$, the diffuse spectrum of UHECR has an universal (standard) form independent of mode of propagation.

For the realistic intergalactic magnetic fields the spectrum is always universal, as was used in this paper.

The most probable astrophysical sources of UHECR are AGN. They can accelerate particles to $E_{\rm max} \sim 1 \times 10^{21}$ eV and provide the needed emissivity of UHECR $\mathcal{L}_0 \sim 3 \times 10^{46}$ erg/Mpc^{3}yr. The correlation of UHE particles with directions to special type of AGN, Bl Lacs, is found in analysis of work [16].

The UHECR from AGN have a problem with superGZK particles with energies $E > 1 \times 10^{20}$ eV: (i) another component is needed for explanation of the AGASA excess, and (ii) no sources are observed in AGASA and other arrays in direction of superGZK particles. UHECR from SHDM can be one of the models explaining supeGZK particles (see Fig. 7 for description of the AGASA excess).

References

[1] K. Greisen, Phys. Rev. Lett., 16, 748 (1966); G.T. Zatsepin, V.A. Kuzmin, Pisma Zh. Experim. Theor. Phys. 4, 114 (1966).

[2] V.S. Berezinsky and S.I. Grigorieva, Astron.Astroph. 199, 1 (1988).

[3] C.T. Hill and D.N. Schramm, Phys. Rev. D 31, 564 (1985).

[4] S. Yoshida and M. Teshima, Progr. Theor. Phys. 89, 833 (1993).

[5] T. Stanev, R.Engel, A.Muecke, R.J. Protheroe and J.P. Rachen, Phys. Rev. D 62, 093005 (2000).

[6] A.V. Glushkov et al (Yakutsk collaboration) JETP Lett. 71, 97 (2000).

[7] A. Watson, these Proceedings.

[8] K.-H. Kampert et al (KASCADE collaboration) Proc. 27th ICRC, volume Invited, Rapporteur and Highlight papers, 240 (2001).

[9] V. Berezinsky, S. Grigorieva and B. Hnatyk, astro-ph/0403477 to be published in Astroparticle Physics.

[10] P.L. Biermann et al, 2003, astro-ph/0302201.

[11] G. Archbold and P.V. Sokolsky, Proc. of 28th ICRC, 405 (2003).

[12] P.L. Biermann P.L. and P.A. Streitmatter, Ap. J., 322, 643 (1987).

[13] W.H. Ipp and W.I. Axford, Astrophysical Aspects of Most Energetic Cosmic Rays (ed. M. Nagano), World Scientific, 273 (1991).

[14] J.P. Rachen and P.L. Biermann, Astron. Astroph. 272, 161 (1993).

[15] V. Berezinsky, A.Z. Gazizov and S.I. Grigorieva, hep-ph/0204357.

[16] P.G. Tinyakov and I.I. Tkachev I.I., JETP Lett., 74, 445 (2001).

[17] V. Berezinsky, A.Z. Gazizov and S.I. Grigorieva, astro-ph/0210095.

[18] V.A. Kuzmin and I.I. Tkachev, Phys. Rep. 320, 199 (199); V. Berezinsky, Nucl. Phys. (Proc. Suppl.) B87, 387 (2000).

[19] R. Aloisio, V. Berezinsky and M. Kachelriess, Phys. Rev. D69, 094023 (2004).

[20] R. Aloisio and V. Berezinsky, astro-ph/0403095 to be published in Ap.J 2004.